Raman scattering of carbon disulfide: The temperature effect

Dake Wang,[a] Kathryn Mittauer, and Nicholas Reynolds
Department of Physics, Furman University, Greenville, South Carolina 29613

(Received 26 March 2009; accepted 21 August 2009)

A low-cost Raman system was constructed and used to perform Raman scattering measurements on liquid carbon disulfide at different sample temperatures. The ν_1 and ν_3 bands are identified based on the frequencies calculated by the normal mode analysis. The ratio of the intensities of the anti-Stokes and Stokes bands can be used to illustrate the Boltzmann distribution of the molecules among the vibrational energy levels. © *2009 American Association of Physics Teachers.*
[DOI: 10.1119/1.3226562]

I. INTRODUCTION

Raman scattering is an inelastic light scattering process in which the energy of the photon is modified by an amount determined by the internal vibrational frequencies of the molecules in the sample. Because each molecule has its own unique set of vibrational modes, spectroscopic techniques based on Raman scattering are capable of identifying unknown substances. Much information on the internal structure of a system such as the symmetry and bond strength of individual molecules can be obtained based on the intensities, frequencies, and widths of the Raman bands. Also, various external factors such as temperature and pressure often have a significant effect on Raman spectra. Because the interpretation of a spectrum relies on understanding various aspects of light-matter interaction, Raman scattering can be used in a capstone experiment for an advanced undergraduate laboratory.

Once lasers became available to serve as the light source for the Raman excitation, Raman spectroscopy was introduced into teaching laboratories.[1–4] With the advent of new generations of diode lasers, more compact spectrometers and charge-coupled-device (CCD)-based detectors, as well as the decrease in the cost of hardware, Raman spectroscopy has increasingly been adapted for undergraduate physics and spectroscopy laboratories.[5–11]

Spontaneous Raman scattering is an inherently weak process (the intensity of scattered light is typically a factor of 10^8 smaller than that of the excitation light),[12] making the observation of Raman spectra challenging. As such, the goals of Raman experiments in undergraduate laboratories are usually limited to the collection and observation of the Raman spectra. Although an introduction to Raman scattering theory based on a continuum dielectric model is usually presented, it is rarely used for the subsequent quantitative analysis of the data gathered by students. Because the quantitative comparison of experimental data to a theoretical model is essential for enhancing the students' overall understanding, it is desirable to establish a closer connection between theory and experiment when designing Raman scattering experiments for teaching laboratories.

The Raman experiment presented in this paper focuses on the temperature dependence of Raman scattering. This dependence can be observed in a number of materials using equipment readily available in most teaching laboratories. The theoretical analysis employs models based on core concepts in classical and statistical mechanics, including modeling a molecule by a spring-mass-system and applying normal mode analysis to determine the frequency and pattern of the oscillations. The scattering processes are described in terms of transitions among vibrational energy levels, relating the intensity of the scattered light to the molecular populations in each energy level.

A Raman scattering system was constructed to observe Raman scattering in liquid carbon disulfide (CS_2). Normal mode analysis of the stretching vibration along the axis of CS_2 provides information on the vibrational frequencies and is used to identify some of the experimentally observed Raman bands. The Raman scattering experiment was performed at different sample temperatures with both Stokes and anti-Stokes scattered light collected. The relative intensities of the anti-Stokes and Stokes bands at different sample temperatures were analyzed based on the Boltzmann distribution of the CS_2 molecules among the ground and excited vibrational states.

II. THEORY

A. The normal modes

CS_2 is a linear molecule belonging to the $D_{\infty h}$ point group.[13] There are $3N$ degrees of freedom for a molecule of N atoms. Excluding the degrees of freedom associated with translational motion of the center of mass and rotational motions, there are $3N-5$ internal vibrational modes for a linear molecule. For a CS_2 molecule there are four normal vibrational modes, among which only the symmetric stretching mode is Raman active. The asymmetric stretching and bending modes are only infrared active.[13]

The atomic displacements of CS_2 in the stretching vibrations measured from the equilibrium positions can be represented by three coordinates, as shown in Fig. 1. Let k be the force constant corresponding to the covalent bonding so that the potential energy V and kinetic energy T can be written as

$$V = \tfrac{1}{2}k[(x_2 - x_1)^2 + (x_3 - x_2)^2], \tag{1}$$

$$T = \tfrac{1}{2}m_1\dot{x}_1^2 + \tfrac{1}{2}m_2\dot{x}_2^2 + \tfrac{1}{2}m_3\dot{x}_3^2. \tag{2}$$

It is more convenient to write the equation of motion in terms of the generalized coordinates q_i,

$$\frac{d}{dt}\left(\frac{\partial T}{\partial \dot{q}_i}\right) + \frac{\partial V}{\partial q_i} = 0, \tag{3}$$

where $q_i = \sqrt{m_i}x_i$. For a normal mode vibration, all the nuclei move at the same frequency ν and with the same phase δ but with different amplitudes A_i,[14]

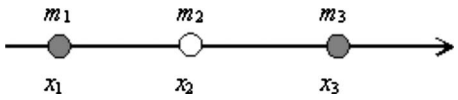

Fig. 1. Coordinates of the atomic displacements measured from the equilibrium positions in a CS_2 molecule. The x-coordinate of the carbon atom is x_2, and those of the sulfur atoms are x_1 and x_3.

$$q_i = A_i \sin(\nu t + \delta). \tag{4}$$

Equations (1)–(4) yield a secular equation that allows the determination of the vibrational frequency ν,

$$\begin{vmatrix} \frac{k}{m_1} - \nu^2 & -\frac{k}{\sqrt{m_1 m_2}} & 0 \\ -\frac{k}{\sqrt{m_1 m_2}} & \frac{2k}{m_2} - \nu^2 & -\frac{k}{\sqrt{m_2 m_3}} \\ 0 & -\frac{k}{\sqrt{m_2 m_3}} & \frac{k}{m_3} - \nu^2 \end{vmatrix} = 0. \tag{5}$$

It is straightforward to write Eq. (5) as a quadratic equation for ν^2,

$$\nu^4 - k\left(\frac{1}{m_1} + \frac{2}{m_2} + \frac{1}{m_3}\right)\nu^2 + k^2\left(\frac{1}{m_1 m_2} + \frac{1}{m_1 m_3} + \frac{1}{m_2 m_3}\right) = 0. \tag{6}$$

The frequencies of the stretching modes can be calculated from Eq. (6), with the two roots corresponding to symmetric and asymmetric stretching: $\nu = \sqrt{k/m_1}$ for symmetric and $\nu = \sqrt{k(1/m_1 + 2/m_2)}$ for asymmetric. We have assumed that the two sulfur atoms have the same mass: $m_1 = m_3$, which is justified by the fact that the $^{12}C\ ^{32}S_2$ isotope is much more abundant than the $^{12}C^{32}S^{34}S$ form.[15]

B. Temperature dependence

The frequencies and linewidths of the Raman bands are often affected by the sample temperature such that the Raman bands usually shift to lower frequencies and become broader with increasing temperature.[16,17] Within the temperature range we used, no significant change in the frequencies or linewidths was observed for the first-order Raman bands of liquid CS_2.

We examined the effect of temperature on the Stokes and anti-Stokes scattering intensities, which is directly related to the population distribution of molecules among the vibrational energy levels. As illustrated in Fig. 2, when a photon is scattered by a molecule in the ground state, its frequency will decrease, and the molecule is promoted to an excited state. Alternatively, the frequency of the photon will increase if it is scattered by a molecule that is in an excited state, with the molecule giving up energy and returning to the ground state. The frequencies of the scattered photons should satisfy $\nu_S = \nu_0 - \nu_P$ for Stokes scattering and $\nu_{AS} = \nu_0 + \nu_P$ for anti-Stokes scattering, where ν_P is the frequency of the vibrational mode and ν_0 is the frequency of the incident light.

The rate of spontaneous Raman scattering depends on the frequency of the photons and the number of molecules available for the Raman transitions,[1,18]

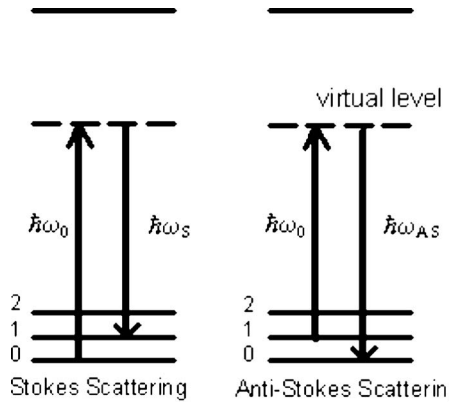

Fig. 2. The energy levels labeled from 0 to 2 correspond to three lowest vibrational energy levels of an electronic state. Shown are the Raman transitions $0 \rightarrow 1$ for Stokes scattering and $1 \rightarrow 0$ for anti-Stokes scattering. Although a transition like $1 \rightarrow 2$ can also generate the same Stokes scattering if the molecules behave like harmonic oscillators, the smaller number of molecules available at higher levels makes this transition less important than the $0 \rightarrow 1$ transition. The same reasoning applies to anti-Stokes scattering.

$$S_{S,AS} \propto \nu_{S,AS}^4 n_{S,AS}. \tag{7}$$

The rate of Stokes scattering S_S is proportional to the population of molecules in the ground state n_S, and the rate of anti-Stokes scattering S_{AS} depends on the population in the excited state n_{AS}. Fewer molecules will be in the excited state, as dictated by Maxwell–Boltzmann statistics,[1,19]

$$\frac{n_i}{n_j} = \exp\left(-\frac{E_i - E_j}{k_B T}\right), \tag{8}$$

where T is the temperature and k_B is Boltzmann's constant. E_i and E_j are the energies of the ith and jth levels,

$$|E_i - E_j| = h\nu_P. \tag{9}$$

Equations (8) and (9) yield the ratio of the molecular population in the excited state to the ground state. The efficiency ratio of the anti-Stokes to Stokes scattering, which is also the intensity ratio of the scattered light, can be readily obtained from Eq. (7) as

$$\frac{S_{AS}}{S_S} = \left(\frac{\nu_{AS}}{\nu_S}\right)^4 \exp\left(-\frac{h\nu_P}{k_B T}\right). \tag{10}$$

The intensities of the scattered light measured in the experiment also depend on the sample absorption, as well as the spectral response of the instrument. If we take these effects into account, Eq. (10) is modified as[20,21]

$$\frac{S_{AS}}{S_S} = \gamma\frac{\alpha_0 + \alpha_{AS}}{\alpha_0 + \alpha_S}\left(\frac{\nu_{AS}}{\nu_S}\right)^4 \exp\left(-\frac{h\nu_p}{k_B T}\right), \tag{11}$$

where $\alpha_0, \alpha_S, \alpha_{AS}$ are the absorption coefficients for the laser, Stokes, and anti-Stokes lights, respectively; γ describes the relative detection efficiency of the instrument at the two frequencies.

All the prefactors of the exponential term in Eq. (11) depend on the frequencies of the scattered light but not on the temperature. Thus, they can be replaced by a single frequency-dependent parameter $F(\nu_{AS}, \nu_S)$, and Eq. (11) can be written as

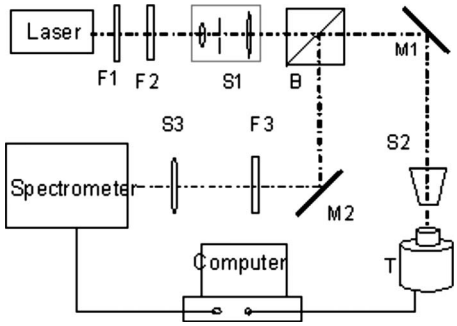

Fig. 3. Schematic diagram of the Raman spectroscopy system. F1, F2, and F3 are a neutral density filter, interference filter, and Raman notch filter, respectively. B is the beam splitter. M1 and M2 are mirrors. S1, S2, and S3 are a beam expander, objective, and achromatic doublet, respectively. T is the TE temperature stage with the sample container placed on top of it.

$$\frac{S_{\mathrm{AS}}}{S_S} = F(\nu_{\mathrm{AS}}, \nu_S) \exp\left(-\frac{h\nu_p}{k_B T}\right), \tag{12}$$

which includes the influence of the temperature on the ratio of scattering intensities to be analyzed in a straightforward fashion.

III. EXPERIMENT

The light source of the Raman spectrometer shown in Fig. 3 was a diode-pumped-solid-state laser emitting at a wavelength of 532 nm in continuous-wave mode. The laser beam was deflected by a 50/50 beam splitter toward an infinity-corrected microscope objective (Nikon, 20×), which focused the excitation laser beam down to a diameter of ~30 μm. The back scattering geometry allowed the scattered light to be collected by the same objective. Because the scattered light is emitted in all directions in spontaneous Raman scattering, it is advantageous to use an objective or lens with a large numerical aperture.[22,23]

A notch filter (Semrock) was employed to reject the Rayleigh-scattered light. The frequency shifted component was focused into the spectrometer (Ocean Optics HR4000) by an achromatic doublet with a focal length of 50 cm, which matched the f-number of the spectrometer. The polarization states of the scattered light were not analyzed in this experiment.

The experimental apparatus shown in Fig. 3 does not necessarily represent the optimal design. The apparatus can be made simpler by collecting the scattered light directly from the sample in a 180° geometry to the spectrometer as discussed in Ref. 9.

At the heart of the spectrometer is a CCD detector with 3648×1 pixels and a 1200 line/mm diffraction grating. The light was focused onto the entrance slit of the spectrometer. With a 50 μm entrance slit, the spectral resolution of the spectrometer is ~0.3 nm, which is equivalent to ~11 cm^{-1} in the vicinity of laser wavelength. A calibration lamp (Oriel) was placed at the sample location, and its emission lines were collected using the same setup. The measured emission line shape gives the spectral point-spread-function of the instrument, which was subsequently employed to deconvolute the measured Raman spectra with the aid of the MATLAB routine deconvreg.

2 ml of liquid CS_2 was placed in a beaker on a hand-built thermoelectric temperature stage. The stage consists of a Peltier module supported by a liquid cooling system and was capable of lowering the sample temperature to −40 °C. A thermistor was submerged in the liquid CS_2 to monitor its temperature.

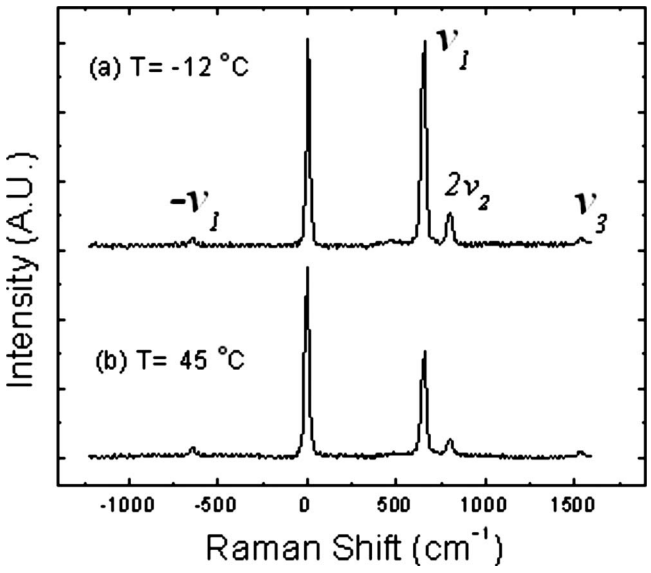

Fig. 4. Raman scattering spectra of liquid CS_2 collected at two temperatures. ν_1 and $-\nu_1$ are Stokes and anti-Stokes Raman lines for symmetric stretching of the molecule, and the unshifted band is due to Rayleigh scattering. The spectra are normalized using the intensity of the anti-Stokes band and displaced vertically for clarity.

Many substances with strong Raman bands can be employed to investigate the temperature dependence provided that they do not undergo a phase change within the temperature range of interest, but practical considerations favored the use of CS_2 for this investigation. Although the frequency shift in the ν_1 Raman band (~655 cm^{-1}) of CS_2 is large enough to distinguish the Raman scattered light from the intense Rayleigh-scattered light, it is low enough for the corresponding anti-Stokes band to have significant intensity at room temperature or lower. As seen in Eq. (10), the anti-Stokes to Stokes ratio decreases exponentially with frequency ν_P, making the observation of anti-Stokes Raman bands beyond 2000 cm^{-1} very difficult.

To avoid any heating of the sample by the focused laser beam, neutral density filters were used to reduce the laser power level. The anti-Stokes to Stokes ratio was observed to decrease with decreasing power levels until the power level (~20 mW at the laser head) was reached, below which the ratio no longer changed. This power level was then used for the collection of experimental data.

IV. RESULT AND CONCLUSION

The Raman spectra of liquid CS_2 were collected at sample temperatures ranging from −30 to 45 °C, with the highest temperature being close to the boiling point of CS_2. Two representative spectra are shown in Fig. 4. The band exhibiting no Raman shift is the Rayleigh scattering band of the laser line, and the strong band at around 655 cm^{-1} is due to the symmetric stretching mode (ν_1) of the molecule. Next to the ν_1 band at around 800 cm^{-1} is the overtone of the bending mode (ν_2). This band is labeled as $2\nu_2$ because its frequency is roughly twice that of the ν_2 mode. The weak band

Table I. The vibrational frequencies of the stretching modes ν_1 and ν_3. The theoretical values are calculated using the normal mode analysis.

	Symmetric ν_1 (cm^{-1})	Asymmetric ν_3 (cm^{-1})
Theory	656	1522
Experiment	655	1525

at around 1525 cm^{-1} is due to the asymmetric stretching mode (ν_3). The assignment of the ν_1 and ν_3 Raman bands is based on the normal mode calculation. The calculated and measured frequencies of the stretching modes are listed in Table I. The calculated values are obtained by choosing the force constant k to be 8.1 md/Å for the ν_1 mode and 6.9 md/Å for the ν_3 mode.[24] The change in the stiffness of a bond resulting from the distortion of other bonds is not a prediction of the classical theory presented here but a result of the quantum mechanical resonance.

The Raman inactive ν_3 band is present because of two factors. One is the lower symmetry of the $^{12}C^{32}S^{34}S$ isotopic form, which allows their asymmetric stretching mode to be Raman active. The other and more important factor is the intermolecular interaction in the liquid, making the inactive modes of isolated molecules weakly allowed.[25,26] The same reasoning can be applied to explain the presence of the bending mode (ν_2), which is also Raman inactive in isolated $^{12}C\ ^{32}S_2$ molecules.[25,26] However, the relatively large bandwidth (590 cm^{-1}) of the notch filter used in our experiment prevents the ν_2 band from being collected by the spectrometer. Instead, what is observed in the spectra is its overtone: The Raman active $2\nu_2$ band.

The only anti-Stokes Raman band observed is that of the symmetric stretching mode. For comparison, the two Raman spectra in Fig. 4 are normalized using the intensity of this anti-Stokes band. It is evident from Fig. 4 that the ratio of the intensities of the anti-Stokes to Stokes band increases with increasing temperature. The spectrally integrated intensities of the anti-Stokes and Stokes bands are determined from the deconvoluted Raman spectra, and the results are given in Fig. 5. A fit of the data in Fig. 5 using Eq. (12) yields the two fitting parameters $F=1.55$ and $\nu_P=658$ cm^{-1}. The vibrational frequency ν_P agrees with the frequency of the symmetric stretching mode, whose Stokes and anti-Stokes bands are employed in the analysis. Therefore, the fit directly validates the theoretical description of the effect of temperature on Raman scattering.

The frequencies of the Raman bands collected at different sample temperatures were also investigated. The data show that the frequency of the $2\nu_2$ band increased slightly with increasing temperature and that of the ν_1 band remained more or less the same within the temperature range of the experiment: The latter is crucial to the use of Eq. (12) in the curve fits.

In summary, a CCD-detector-based Raman scattering system was constructed to perform Raman scattering measurement of liquid CS_2 at sample temperatures ranging from −30 to 45 °C. The ν_1, $2\nu_2$, and ν_3 bands are present in the Raman spectra, and anti-Stokes part of the ν_1 band is also observed. The ν_1 and ν_3 bands are identified based on the frequencies calculated by the normal mode analysis of the stretching vibration. Curve fits reveals that the ratio of the intensities of the anti-Stokes to Stokes band obtained at different sample temperatures is well described by the Boltzmann distribution of the CS_2 molecules between their ground and excited vibrational states. The effect of temperature on the Raman scattering of liquid CS_2 discussed thus lends itself to a straightforward comparison between the theoretical analysis and experimental measurements and is well suited for the advanced undergraduate laboratory.

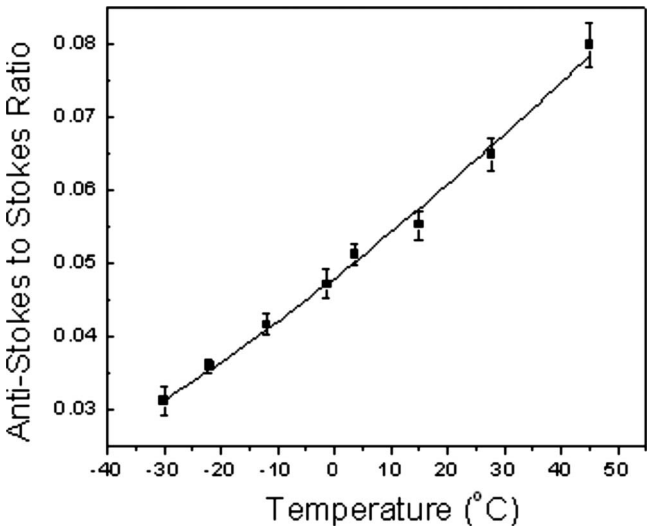

Fig. 5. The ratio of the intensities of the anti-Stokes $-\nu_1$ to Stokes ν_1 band versus the sample temperature. The dots are the measured values, and the solid curve is the curve fitting based on Eq. (12). Error bars are associated with the systematic errors resulted from the spectral line broadening of the instrument.

ACKNOWLEDGMENTS

Two of the authors (K.M. and N.R.) would like to acknowledge the financial support from Furman University through Furman Advantage Research Fellowships. The authors would like to thank the reviewers for providing helpful comments and advice.

[a]Electronic mail: dake.wang@furman.edu

[1] B. R. Fugitt and A. S. Rupaal, "Raman spectroscopy experiment for the senior laboratory," Am. J. Phys. **36**, 17–23 (1968).
[2] D. F. Edwards and C. Y. She, "Laser-excited Raman spectroscopy," Am. J. Phys. **40**, 1389–1399 (1972).
[3] R. Feinberg, "A simple apparatus for observing the Raman effect," Am. J. Phys. **58**, 893–893 (1989).
[4] A. Compaan, A. Wagoner, and A. Aydinli, "Rotational Raman scattering in the instructional laboratory," Am. J. Phys. **62**, 639–645 (1994).
[5] D. Cleveland, M. Carlson, E. D. Hudspeth, L. E. Quattrochi, K. L. Batchler, S. A. Balram, Seongun Hong, and R. G. Michel, "Raman spectroscopy for the undergraduate teaching laboratory: Quantification of ethanol concentration in consumer alcoholic beverages and qualitative identification of marine diesels using a miniature Raman spectrometer," Spectrosc. Lett. **40**, 903–924 (2007).
[6] B. L. Sands, M. J. Welsh, S. Kin, R. Marhatta, J. D. Hinkle, and S. B. Bayram, "Raman scattering spectroscopy of liquid nitrogen molecules: An advanced undergraduate physics laboratory experiment," Am. J. Phys. **75**, 488–495 (2007).
[7] P. Bisson, G. Parodi, D. Rigos, and J. E. Whitten, "Low-cost Raman spectroscopy using a violet diode laser," Chem. Educ. **11**(2), 1–6 (2006), ⟨chemeducator.org/sbibs/s0011002/spapers/1120088jw.htm⟩.
[8] E. D. Hudspeth, D. C. Kathleen, L. Batchler, P. A. Nguyen, T. L. Feaser, L. E. Quattrochi, J. Morenz, S. A. Balram, and R. G. Michel, "Teaching Raman spectroscopy in both the undergraduate classroom and the labo-

ratory with a portable Raman instrument," Spectrosc. Lett. **39**, 99–115 (2006).
[9] A. Singha, P. Dhar, and A. Roy, "A nondestructive tool for nanomaterials: Raman and photoluminescence spectroscopy," Am. J. Phys. **73**, 224–233 (2005).
[10] G. A. Lorigan, B. M. Patterson, A. J. Sommer, and N. D. Danielson, "Cost-effective spectroscopic instrumentation for the physical chemistry laboratory," J. Chem. Educ. **79**, 1264–1266 (2002).
[11] R. Voor, L. Chow, and A. Schulte, "Micro-Raman spectroscopy in the undergraduate research laboratory," Am. J. Phys. **62**, 429–434 (1994).
[12] T. R. Gilson and P. J. Hendra, *Laser Raman Spectroscopy* (Wiley, London, 1970), pp. 9–12.
[13] M. S. Dresselhaus, G. Dresselhaus, and A. Jorio, *Group Theory: Application to the Physics of Condensed Matter* (Springer-Verlag, Berlin, 2008), pp. 164–165.
[14] K. Nakamoto, *Infrared and Raman Spectra of Inorganic and Coordination Compounds*, 4th ed. (Wiley, New York, 1986), pp. 12–17.
[15] Sulfur isotope data are from The Berkeley Laboratory Isotopes Project, ⟨ie.lbl.gov/education/parent/S_iso.htm⟩.
[16] W. S. Li, Z. X. Shen, Z. C. Feng, and S. J. Chua, "Temperature dependence of Raman scattering in hexagonal gallium nitride films," J. Appl. Phys. **87**, 3332–3337 (2000).
[17] K. A. Alim, V. A. Fonobeov, and A. A. Balandin, "Origin of the optical phonon frequency shifts in ZnO quantum dots," Appl. Phys. Lett. **86**, 053103-1–3 (2005).
[18] A. B. F. Duncan and A. Weissberger, *Technique of Organic Chemistry* (Interscience, New York, 1944), Vol. 9, p. 198.
[19] C. Kittel, *Introduction to Solid State Physics*, 7th ed. (Wiley, New York, 1996), pp. 117–118.
[20] M. Balkanski, R. F. Wallis, and E. Haro, "Anharmonic effects in light scattering due to optical phonons in silicon," Phys. Rev. B **28**, 1928–1934 (1983).
[21] D. Wang, M. Park, Y. N. Saripalli, M. A. L. Johnson, C. Zeng, D. W. Barlage, and J. P. Long, "Optical spectroscopic analysis of selected area epitaxially re-grown n^+ GaN," J. Appl. Phys. **99**, 123106-1–6 (2006).
[22] *Practical Raman Spectroscopy*, edited by D. J. Gardiner and P. R. Graves (Springer-Verlag, Berlin, 1989), p. 27.
[23] R. L. McCreery, *Raman Spectroscopy for Chemical Analysis* (Wiley, New York, 2000), pp. 108–109.
[24] E. B. Wilson, Jr., J. C. Decius, and P. C. Cross, *Molecular Vibrations: The Theory of Infrared and Raman Vibrational Spectra*, revised edition (Dover, New York, 1980), pp. 177–178.
[25] S. Ikawa and E. Whalley, "Polarized and depolarized Raman spectra of liquid carbon disulfide at 0–10 kbar. 3. Interaction-induced v_2 and v_3 scattering and the fluctuation of the local field," J. Phys. Chem. **94**, 7834–7839 (1990).
[26] J. C. Evans and H. J. Bernstein, "Intensity in the Raman effect. V. The effect of intermolecular interaction on the Raman spectrum of carbon disulfide," Can. J. Chem. **34**, 1127–1133 (1956).

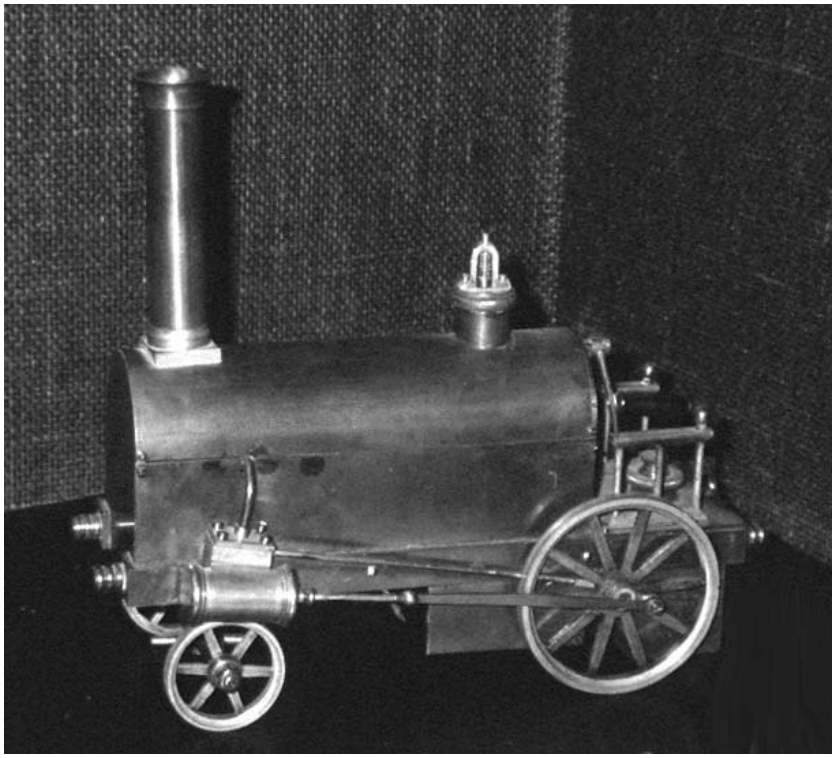

Brass Locomotive Model. This live steam locomotive model was used for demonstrations at Vanderbilt University in the last years of the nineteenth century. The nineteenth century physics course often included examples of applied technology, including steam engines. Lagemann (*The Garland Collection of Classical Physics Apparatus at Vanderbilt University*, Nashville, 1983) notes that the model was probably made in France, and that its front wheels could be set at an angle to make it run in circles on the lecture table. (Photograph and Notes by Thomas B. Greenslade, Jr., Kenyon College)